Molecular Biology of the Cell
Vol. 13, 2706–2717, August 2002

Fluorescence Resonance Energy Transfer Detection of Synaptophysin I and Vesicle-associated Membrane Protein 2 Interactions during Exocytosis from Single Live Synapses

Maria Pennuto,* David Dunlap,* Andrea Contestabile,* Fabio Benfenati,† and Flavia Valtorta*‡

*Department of Neuroscience, S. Raffaele Scientific Institute and "Vita-Salute" University, Milan, Italy; and †Department of Experimental Medicine, Section of Human Physiology, University of Genoa, Italy

Submitted January 22, 2002; Revised March 28, 2002; Accepted May 7, 2002
Monitoring Editor: Hugh R.B. Pellham

To investigate the molecular interactions of synaptophysin I and vesicle-associated membrane protein 2 (VAMP2)/synaptobrevin II during exocytosis, we have used time-lapse videomicroscopy to measure fluorescence resonance energy transfer in live neurons. For this purpose, fluorescent protein variants fused to synaptophysin I or VAMP2 were expressed in rat hippocampal neurons. We show that synaptophysin I and VAMP2 form both homo- and hetero-oligomers on the synaptic vesicle membrane. When exocytosis is stimulated with α-latrotoxin, VAMP2 dissociates from synaptophysin I even in the absence of appreciable exocytosis, whereas synaptophysin I oligomers disassemble only upon incorporation of the vesicle with the plasma membrane. We propose that synaptophysin I has multiple roles in neurotransmitter release, regulating VAMP2 availability for the soluble *N*-ethylmaleimide-sensitive factor attachment protein receptor complex and possibly participating in the late steps of exocytosis.

INTRODUCTION

Neurotransmitter release comprises a series of steps involving synaptic vesicle (SV), plasma membrane, and cytosolic proteins. The molecular characterization of the repertoire of proteins involved has been the goal of a large body of experimental work (reviewed by Südhof, 1995; Valtorta and Benfenati, 1995; Benfenati *et al.*, 1999; Valtorta *et al.*, 2001). Although a large number of proteins involved in exocytosis have been identified and many interactions among them have been characterized in vitro, the precise physiological role(s) of most of them have not yet been clearly demonstrated.

Article published online ahead of print. Mol. Biol. Cell 10.1091/mbc.E02–01–0036. Article and publication date are at www.molbiolcell.org/cgi/doi/10.1091/mbc.E02–01–0036.

‡ Corresponding author. E-mail address: valtorta.flavia@hsr.it.

Abbreviations used: Cyt, cytoplasmic; DIV, days in vitro; ECFP, enhanced cyano fluorescent protein; EYFP, enhanced yellow fluorescent protein; FRET, fluorescence resonance energy transfer; KRH, Krebs-Ringer-HEPES; α-Ltx, α-latrotoxin; SNARE, soluble *N*-ethylmaleimide-sensitive factor attachment protein receptor; SV, synaptic vesicle; SV2, synaptic vesicle protein 2; SypI, synaptophysin I; SytI, synaptotagmin I; VAMP2, vesicle-associated membrane protein 2/synaptobrevin II.

A typical example is synaptophysin I (SypI), one of the first SV proteins to be identified (Jahn *et al.*, 1985; Wiedenmann and Franke, 1985). SypI is an abundant SV protein characterized by four membrane-spanning domains (Buckley *et al.*, 1987; Leube *et al.*, 1987; Südhof *et al.*, 1987). In vitro, SypI has been shown to form homo-oligomers composed of a variable number of subunits (Jahn *et al.*, 1985; Rehm *et al.*, 1986) that, when incorporated into lipid bilayers, form voltage-dependent channels with a conductance similar to that of gap junctions (Thomas *et al.*, 1988). Although SypI and the gap junction protein connexin share little sequence homology, the two proteins have similar membrane topologies and amino acid compositions of the third transmembrane domain, which, in connexin, lines the gap junction pore (Leube, 1995).

Apparently contradictory data have been reported concerning the role of SypI in neurotransmitter release. Antisense oligonucleotides or antibodies directed against SypI drastically reduced evoked release reconstituted in *Xenopus* oocytes (Alder *et al.*, 1992a; Shibaguchi *et al.*, 2000). Consistently, antibodies to SypI reduced, and SypI overexpression enhanced, acetylcholine release from *Xenopus* motor spinal neurons (Alder *et al.*, 1992b, 1995). In contrast, SypI overexpression decreased the secretion of growth hormone transfected in PC12 cells (Sugita *et al.*, 1999). SypI knockout mice exhibited an apparently normal phenotype (Eshkind and

Leube, 1995; McMahon *et al.*, 1996), raising the possibility that other isoforms of the synaptophysin family (Knaus *et al.*, 1990; Leube, 1994), or related proteins, such as the synaptogyrins (Baumert *et al.*, 1990; Janz and Südhof, 1998), can compensate for the lack of SypI. Indeed, SypI/synaptogyrin I double knockout mice showed defects in both short- and long-term potentiation (Janz *et al.*, 1999).

SypI interacts in vitro with several SV proteins, including the v-soluble *N*-ethylmaleimide-sensitive factor attachment protein receptor (SNARE) vesicle-associated membrane protein 2 (VAMP2)/synaptobrevin II (Calakos and Scheller, 1994; Edelmann *et al.*, 1995; Washbourne *et al.*, 1995) as well as with lipids, such as cholesterol (Thiele *et al.*, 2000). VAMP2 is an integral SV protein (Baumert *et al.*, 1989; Elferink *et al.*, 1989), which interacts with the plasma membrane proteins syntaxin 1A and soluble *N*-ethylmaleimide-sensitive factor attachment protein-25 to form a complex (the SNARE complex) that drives fusion (Söllner *et al.*, 1993; reviewed by Pelham, 2001). Because the binding of VAMP2 to SypI seems to be mutually exclusive with VAMP2 engagement in the SNARE complex (Edelmann *et al.*, 1995), it is possible that SypI, by sequestering VAMP2, impairs the assembly of SNARE complexes.

The ability of SypI to interact with several SV constituents suggests that it might be involved in multiple functions during the SV cycle. At all these sites, SypI does not seem to act alone but rather to cooperate with other proteins. This could explain why SypI does not seem to be essential for transmitter release but rather to participate in its regulation, playing either a positive (Alder *et al.*, 1992a,b, 1995) or a negative (Sugita *et al.*, 1999) role, depending on the system and the experimental conditions investigated.

In the present study, to overcome the limitations associated with studying protein–protein interactions in vitro, we have used, for the first time, video-enhanced microscopy of living neurons to detect fluorescence resonance energy transfer (FRET) between fluorescent SypI and VAMP2. With this technique, we have investigated the in vivo dynamics of SypI and VAMP2 homo-oligomerization and of SypI-VAMP2 interaction under resting conditions and during exocytosis.

MATERIALS AND METHODS

Generation of Chimeric Fluorescent Proteins

Rat SypI full-length cDNA (921 base pairs) cloned into the pBlueScript vector (Stratagene, La Jolla, CA) was provided by Dr. R. Leube (University of Mainz, Mainz, Germany). SypI cDNA was amplified by polymerase chain reaction (PCR) with the following oligonucleotides: forward, 5′-GGGGGAAGCTTCAGCAGCAATGGACGTG-3′; and reverse, 5′-GGGGGGATCCGCTGCTGTAGTAGCAGTAGGTCTTGGGCTCCACGCCCTTCATCTGATTGGAGAA-GGAGGTGG-3′. *Hin*dIII and *Bam*HI restriction sites, introduced with the forward and reverse primers, respectively, are underlined. The reverse primer was designed to remove the stop codon and, in addition, to introduce a linker of 13 amino acids (KGVEPKTYCYYSS) (Nakata *et al.*, 1998) at the COOH-terminal end of SypI cDNA. The resultant *Hin*dIII/*Bam*HI PCR fragment was inserted into the corresponding sites of pECFP-N3 and pEYFP-N3 vectors (CLONTECH, Palo Alto, CA).

The COOH-terminal deletion mutant of SypI (702 base pairs), lacking the last 73 amino acids of the protein and fused to the enhanced green fluorescent protein (EGFP) in the pEGFP-N3 vector (CLONTECH), was also provided by Dr. R. Leube. The mutated SypI cDNA was digested with *Bam*HI and BsrGI to remove EGFP and replace it with *Bam*HI/BsrGI ECFP and EYFP fragments of pECFP-N3 and pEYFP-N3.

VAMP2 full-length cDNA (351 base pairs) cloned into pBlueScript was from Drs. C. Montecucco and O. Rossetto (University of Padua, Italy). VAMP2 cDNA was amplified by PCR with the following oligonucleotides: forward, 5′-GGGGTGTACAAGATGTCGGCTACCGCTGCCAC-3′; and reverse, 5′-GGGGGCGGCCGCTTAAGTGCTGAAGTAAAC-3′. BsrGI and *Not*I restriction sites, introduced with the forward and reverse primers, respectively, are underlined. The resultant BsrGI/*Not*I PCR fragment was inserted into the corresponding sites of pECFP-N3 and pEYFP-N3.

Synaptotagmin I (SytI) full-length cDNA (1265 base pairs) was supplied by Dr. G. Schiavo (Imperial Cancer Research Fund, London, United Kingdom). After removing the stop codon by PCR, the cDNA was fused to the NH_2-terminal end of EYFP in pEYFP-N3, generating the pSytI-EYFP vector.

Cell Cultures and Transfections

Transfection of Cos-7 cells was performed using a standard Ca^{2+}-phosphate precipitation protocol (Kingston, 1997). Cells were used 72 h after transfection.

Low-density, primary cultures of hippocampal neurons were prepared from Sprague-Dawley E18 rat embryos (Charles River Italica, Calco, Italy) as described previously (Banker and Cowan, 1977). Neurons were transfected at 3 d in vitro (DIV) by using 25-kDa polyethylenimine (PEI 25) (Sigma-Aldrich, Steinheim, Germany). Fresh medium was applied to cell cultures 1 h before starting the procedure. Then, PEI 25 (28 nmol/dish) and plasmid DNA (2.5 μg/dish) were diluted in 50 μl of 150 mM NaCl in separate tubes. The solution containing PEI 25 was added to that containing the DNA, and the mixture was vortexed four times within 12 min before addition to the cells. Coverslips were placed in a clean 35-mm Petri dish and cells were rinsed with minimal essential medium supplemented with 10% horse serum, 2 mM glutamine, and 3.3 mM glucose. The medium was removed and cells were incubated for 2 h at 37°C in a 5% CO_2, humidified atmosphere with 1 ml of the same medium containing the 100 μl of PEI 25/DNA solution. Coverslips were then repositioned above astrocyte monolayers in the original dishes and kept in culture for 15–18 d. Transfection efficiency varied from 0.1 to 1%.

Immunoblot Analysis

Gel electrophoresis and immunoblotting of cell lysates were carried out as described previously (Menegon *et al.*, 2000) with either monoclonal (R. Jahn, Max Planck Institute of Biophysical Chemistry, Göttingen, Germany) or polyclonal (Valtorta *et al.*, 1988) anti-SypI antibodies (1:5000 and 1:3000, respectively), polyclonal anti-VAMP2 antibody (1:500) (C. Montecucco), or monoclonal anti-GFP antibody (Roche Molecular Biochemicals, Indianapolis, IN).

Immunofluorescence Analysis

Immunofluorescence was performed as described previously (Menegon *et al.*, 2000), using the following primary antibodies: monoclonal anti-synaptic vesicle protein 2 (SV2) (1:50) (K. Buckley, Harvard University, Boston, MA), anti-microtubule associated protein-2 (MAP2) (1:1000) (Roche Molecular Biochemicals) and polyclonal anti-SypI or anti-synapsin I (1:100) (Valtorta *et al.*, 1988). In some instances, primary antibodies were applied to unfixed cells in Krebs-Ringer solution buffered with HEPES (150 mM NaCl, 5 mM KCl, 1.2 mM $MgSO_4$, 1.2 mM KH_2PO_4, 2 mM $CaCl_2$, 10 mM glucose, and 10 mM HEPES/Na, pH 7.4) supplemented with 2 mM EGTA (KRH/EGTA). The incubation was carried out for 1 h at 37°C in 5% CO_2. After two washes with KRH/EGTA, samples were fixed and processed for indirect immunofluorescence. Images were recorded with a C4742-98 ORCA II cooled charge-coupled device camera

(Hamamatsu Photonics, Hamamatsu City, Japan) and processed using the computer program ImagePro Plus 4.0 (Media Cybernetics, Silver Spring, MD).

Spectrofluorometric Analysis

Cos-7 cells were transiently transfected with an expression vector encoding one of the chimeric, fluorescent proteins of interest. Seventy-two hours after transfection, the cells were washed twice with phosphate-buffered saline and collected by scraping. The cells were then pelleted by centrifugation, resuspended in 700 μl of phosphate-buffered saline, and analyzed in a spectrofluorometer (LS50B; PerkinElmer, Shelton, CT).

FM1-43 Assay

FM1-43 (8 μM) (Molecular Probes, Eugene, OR) was loaded into recycling SVs of 16 DIV hippocampal neurons by using a depolarizing solution containing KRH supplemented with 45 mM KCl and 10 μM 6-cyano-2,3-dihydroxy-7-nitroquinoxaline. The incubation was carried out for 90 s at room temperature and was followed by rinsing for 15 min with a 2-ml/min flow of KRH containing 6-cyano-2,3-dihydroxy-7-nitroquinoxaline. After the washing protocol, images were recorded using fluorescein excitation and rhodamine emission filters, and a 40× oil immersion objective. Average intensities for each bouton (I_{KRH}) were measured. Cells were then rapidly rinsed with KRH/EGTA and incubated for 40 min at room temperature in the same solution in the absence or presence of 0.1 nM α-latrotoxin (α-Ltx) (A. Petrenko, New York University Medical Center, New York, NY). After 15 s of continuous illumination for focusing on the specimen, a series of 20 images at 6-s intervals were recorded for each of the fields previously acquired. FM1-43 release was calculated by comparing the intensity of fluorescence in each synaptic bouton before and after the incubation. To correct for the reduction in fluorescence intensity due to photobleaching that occurred during the 15-s exposure used for focusing, an exponentially decaying curve of the form $y(t) = Ae^{-t/\tau} + C$ was fit to the average intensity vs. time data for each single synaptic bouton in the sequence of images acquired. This expression was used to calculate a corrected postincubation fluorescence intensity ($I_{KRH/EGTA}$) for each bouton. FM1-43 release was then calculated as $(1 - I_{KRH/EGTA}/I_{KRH})$.

α-Latrotoxin Binding Assay

Anti α-Ltx antibody was purchased from Alomone Laboratories (Jerusalem, Israel), conjugated to Cy3 (Amersham Biosciences, Piscataway, NJ), and purified according to the manufacturer's instructions. Hippocampal neurons of 16 DIV were washed once with KRH/EGTA and incubated for 30 min at 37°C in 5% CO_2 in the same solution supplemented with Cy3-conjugated, anti α-Ltx antibody (50 μg/ml) in the absence or presence of 0.1 nM α-Ltx. The cells were washed twice with KRH/EGTA, and Cy3 images were acquired with a standard Texas Red filter set.

Fluorescence Resonance Energy Transfer (FRET) Analysis

Expression vectors encoding fluorescent proteins were cotransfected at a ratio of 1:2 or 1:4 (donor/acceptor). Cells (15–18 DIV) were washed once with KRH/EGTA and incubated in the same solution either in the presence or absence of 0.1 nM α-Ltx for 30 min at 37°C in 5% CO_2; the cells were then washed twice with KRH/EGTA. Images were acquired within 30–45 min after treatment of the cells. The specimen was irradiated at the wavelength of 436 ± 10 nm, and a time-lapse series of images of the donor fluorescence were recorded at the wavelength of 480 ± 30 nm during continuous illumination. From the first image of the series, a binary mask was prepared, in which each spot corresponded to a synaptic bouton. Fluorescent spots that moved quickly along the axon (and that presumably represented traveling packets) were excluded from the analysis. The time series data for each pixel position within a bouton were fit to an exponential decay function to determine decay constants of photobleaching (Figure 1).

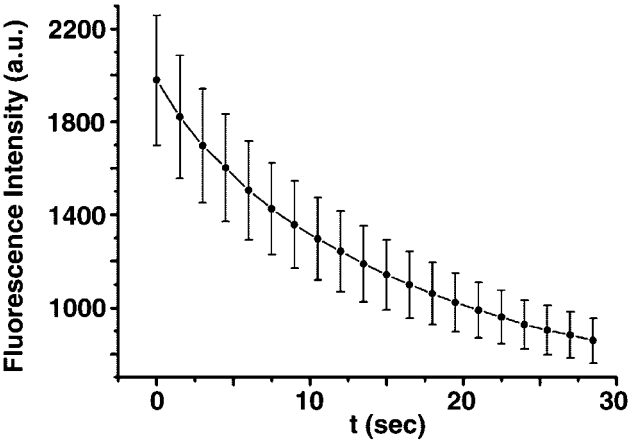

Figure 1. Time course of the decay of donor fluorescence during continuous illumination. The figure shows an example of the fluorescence intensity of SypI-ECFP transfected in hippocampal neurons measured in a series of time-lapse images by using a 12-bit monochrome video camera. Measurements were carried out separately for individual pixels in one field of view (total number of pixels, 634). The intensity values at each time point were averaged and plotted.

When FRET occurs between donor and acceptor fluorophores, the time constant for donor photobleaching increases (Jovin and Arndt-Jovin, 1989). Thus, the efficiency (E) of FRET was calculated as the percentage of change in the average time constant of donor photobleaching measured in specimens transfected with the SV-located acceptor fluorescent proteins (τ_{sv^*sv}), with respect to that measured in specimens transfected with cytosolic EYFP acceptor (τ_{sv^*cyt}) via the following equation: $E = 1 - (\tau_{sv^*cyt}/\tau_{sv^*sv})$.

One of the advantages of this method for measuring FRET is that the measurements do not depend on absolute values of fluorescence. Indeed, we found no significant correlation between initial intensities of fluorescence and photobleaching rates ($R \approx 0.4$). The photobleaching time constants were found to have skewed distributions, which became normal after logarithmic transformation. Therefore, data were analyzed using the natural logarithms of the photobleaching time constants, and efficiencies and statistics were derived by retransformation of the pertinent values. Where indicated, one-tailed *t* tests were performed to estimate the significance of differences between mean FRET efficiencies. To estimate the probability that a given mean FRET efficiency was statistically different from zero, the mean value normalized by the SD of the mean was compared with a one-tailed Z distribution.

RESULTS

Generation and Characterization of Chimeric Fluorescent Proteins SypI and VAMP2

To apply the FRET technique to the study of the molecular interactions occurring during exocytosis, we fused ECFP or EYFP to the SV proteins SypI and VAMP2. The fluorescent proteins were fused to the cytosolic, COOH-terminal tail of SypI, to obtain SypI-ECFP and SypI-EYFP, or to the cytoso-

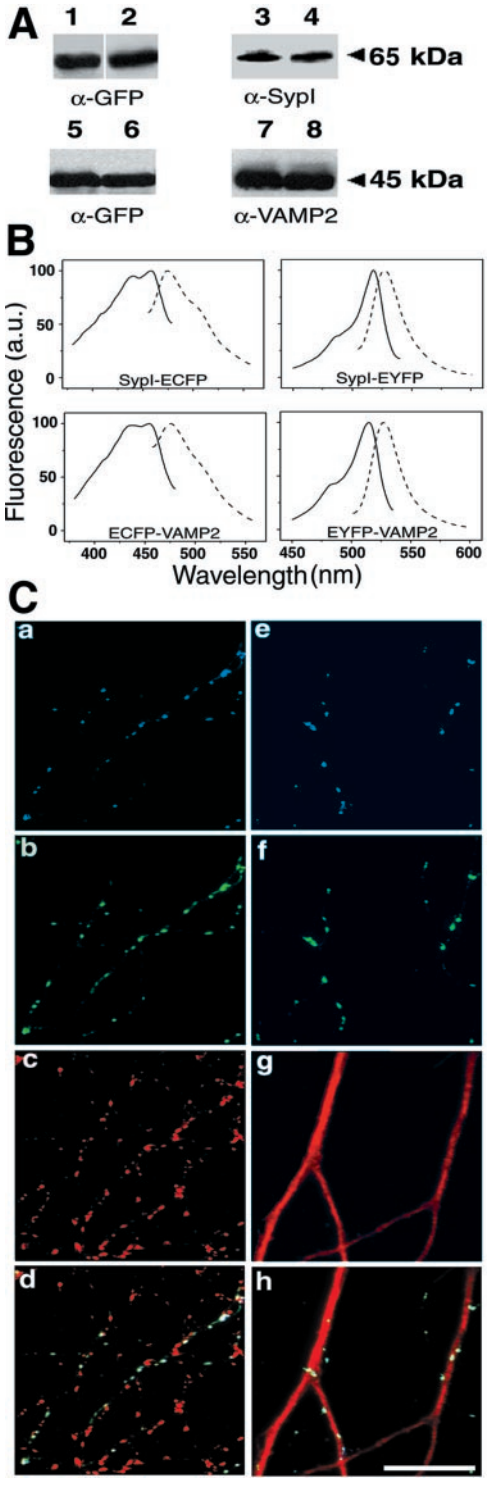

Figure 2. Expression and targeting of the SypI and VAMP2 fluorescent fusion proteins. (A) Fusion proteins are properly translated in the cells. Cos-7 cells were transiently transfected with the expression vectors encoding either SypI-ECFP (lanes 1 and 3), SypI-EYFP (lanes 2 and 4), ECFP-VAMP2 (lanes 5 and 7), or EYFP-VAMP2 (lanes 6 and 8). Seventy-two hours after transfection, cells were analyzed by immunoblotting with anti-green fluorescent protein (lanes 1, 2, 5, and 6) and either anti-SypI (lanes 3 and 4) or anti-VAMP2 (lanes 7 and 8) antibodies. (B) Fusion of the fluorescent proteins to the SV proteins does not alter the spectral properties of the fluorophores. The excitation (solid) and emission (dashed) spectra of the chimeras were measured in suspensions of transiently transfected Cos-7 cells. (C) Exogenous SV fusion proteins are targeted to synaptic boutons in transfected neurons. Hippocampal neurons were cotransfected with the expression vectors encoding SypI-EYFP and ECFP-VAMP2 and processed for immunofluorescence with either anti-SV2 or anti-MAP2 antibodies. (a–d) Colocalization of both ECFP-VAMP2 (a) and SypI-EYFP (b) with SV2 (c), and overlay of a, b, and c (d). (e–h) Lack of colocalization of ECFP-VAMP2 (e) and SypI-EYFP (f) with MAP2 (g), and overlay of e, f, and g (h). Bar, 10 μm.

lic, NH_2-terminal end of VAMP2 to generate ECFP-VAMP2 and EYFP-VAMP2. Chimeras of a SypI deletion mutant lacking the cytosolic, COOH-terminal tail of the protein (SypIΔC-ECFP and SypIΔC-EYFP) were also prepared. In addition, EYFP was fused to the cytosolic, COOH terminus of SytI, to generate SytI-EYFP.

The expression of the full-length fusion proteins was verified in non-neuronal Cos-7 cells transfected with the appropriate vectors (Figure 2A; our unpublished data). In addition, the fusion proteins were shown to exhibit spectral properties similar to those of the soluble fluorophores (Tsien, 1998; Figure 2B; our unpublished data).

Hippocampal neurons were transfected at 3 DIV and kept in culture until 15–18 DIV, which corresponds to full maturation and the establishment of a synaptic network with surrounding cells (Valtorta and Leoni, 1999). We verified the expression and proper targeting of the chimeras, as well as the absence of toxicity related to the sustained, high level of expression. Immunolabeling of neurons cotransfected with the expression vectors encoding ECFP-VAMP2 and SypI-EYFP confirmed that both fusion proteins colocalized with the endogenous SV protein SV2 (Bajjalieh *et al.*, 1994; Figure 2C; our unpublished data). Indeed, the colocalization coefficients of SV2 with ECFP-VAMP2, SypI-ECFP, or SytI-ECFP were 0.88, 0.80, and 0.99, respectively. Furthermore, the exogenous proteins were delivered to axons and did not colocalize with MAP2, which in mature neurons is present exclusively in the somatodendritic compartment (Kosik and Finch, 1987).

No apparent developmental changes due to overexpression of the transfected proteins could be detected. In particular, there were no effects on the density of synapses (4.6 ± 2.4 and 3.8 ± 0.8 synapses/10-μm neurite length in the untransfected and transfected neurons, respectively) nor on the number of synaptic vesicles per terminal (our unpublished data).

Effect of α-Ltx on Synaptic Boutons

To trigger exocytosis, hippocampal neurons at 15–18 DIV were treated with 0.1 nM purified α-Ltx for 30 min in Ca^{2+}-free medium (KRH/EGTA), a condition known to cause massive exocytosis of SVs in the absence of endocytosis (Ceccarelli and Hurlbut, 1980; Valtorta *et al.*, 1988). Video analysis showed that, after a 10-min delay, the morphology of the axons changed progressively, and at the end of the treatment the axons assumed a characteristic bead-shaped

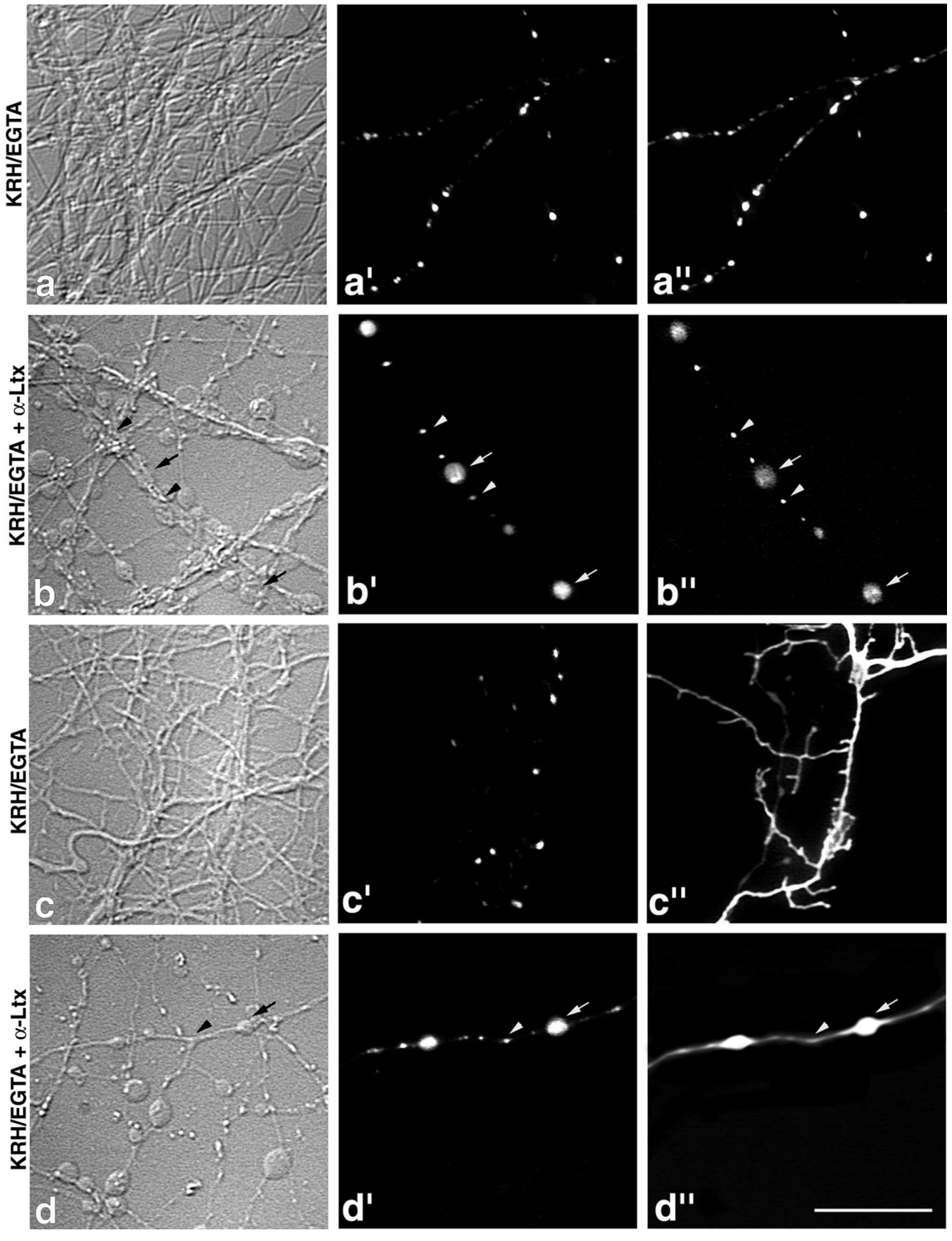

Figure 3. Heterogeneity in the responses of synaptic boutons to α-Ltx. At 15 DIV, hippocampal neurons cotransfected with vectors encoding either ECFP-VAMP2 and SypI-EYFP (a–a″ and b–b″) or SypI-ECFP and EYFP (c–c″ and d–d″) were incubated for 30 min in Ca^{2+}-free medium (KRH/EGTA) in the absence or presence of 0.1 nM α-Ltx. Differential contrast images (a–d), SypI-EYFP (a′ and b′), SypI-ECFP (c′ and d′), ECFP-VAMP2 (a″ and b″), and EYFP (c″ and d″). Note the presence of two distinct classes of synaptic boutons in the toxin-treated samples: one with diameters in the range of those observed in control samples (arrowheads) and the other with considerably larger diameters (arrows). SypI and VAMP2 fluorescent chimeras are present exclusively at synapses, whereas soluble EYFP is distributed throughout the neurites of the transfected cells. Bar, 10 μm.

structure, due to the irreversible, exhaustive fusion of SVs with the plasma membrane, with the consequent swelling of nerve terminals (Ceccarelli and Hurlbut, 1980; Nakata *et al.*, 1998) (Figure 3). In toxin-treated neurons showing the characteristic bead-like appearance of SypI-ECFP, the integrity of the axon was verified by the uniform and continuous distribution of cytosolic EYFP between adjacent beads (Figure 3), as well as by α-tubulin and MAP2 immunostaining (our unpublished data).

In the toxin-treated neurons, the distribution of the fluorescent proteins characterized two populations of synaptic boutons: one population of swollen boutons, and another population of small boutons very similar to those of untreated cells. Indeed, morphometric analysis of fluorescence images revealed a bimodal size distribution of synaptic boutons. The class of swollen boutons comprised 27.1 ± 4.3% (mean ± SEM; number of boutons analyzed, 965 in 10 random fields of view) of the boutons and showed an average fluorescent area of 3.51 ± 0.12 μm^2 (n = 91). The remaining 73.8 ± 5.5% of the boutons were small boutons and showed a fluorescent area of 0.64 ± 0.024 μm^2 (n = 100), a value similar to that observed in untreated samples (0.72 ± 0.02 μm^2; n = 100). When higher concentrations of α-Ltx were used, the percentage of swollen synaptic boutons increased accordingly (our unpublished data).

Quantitative Analysis of α-Ltx-induced SV Exocytosis

To estimate the fraction of vesicles that underwent exocytosis in both the swollen and small boutons, the fluorescent styryl dye FM1-43 (Betz *et al.*, 1996) was loaded into SVs of 16 DIV hippocampal neurons using high K^+ depolarization in a well established protocol that labels the entire pool of recycling vesicles (Pyle *et al.*, 2000). Subsequently, the amount of FM1-43 staining of each single synaptic bouton was evaluated before and after a 40-min incubation of the neurons in Ca^{2+}-free medium in either the absence or presence of α-Ltx (Figure 4).

Under resting conditions, the amount of dye released during the 40-min incubation was estimated to be 24.3 ± 0.7% (mean ± SEM; n = 245) of that initially loaded. In toxin-treated samples, swollen synaptic boutons lost virtually 100% of the loaded dye. The fluorescent areas of swollen synapses ranged between 1.66 and 5.86 μm^2, which correspond to apparent circular radii of 0.727 and 1.36 μm, respectively (these values probably overestimate the actual size of the boutons, because they include the fluorescence halo). Considering resting and small boutons to be spheres and swollen boutons (which show a tendency to partially collapse onto the substrate) to be hemispheres, we estimated that the increase in the surface area of swollen boutons could be accounted for by the fusion of 40–1287 SVs. Because the number of SVs per bouton in 14 DIV hippocampal neurons was found to range from 23 to 648 (Schikorsky and Stevens, 1997), these data are compatible with the idea that the class of large boutons corresponds to synapses in which α-Ltx induced exocytosis of virtually all SVs. In contrast, synapses belonging to the class of small synaptic boutons released 29.7 ± 1.0% (mean ± SEM; n = 220) of the loaded dye, i.e., a fraction only slightly higher than that observed in resting cultures, indicating that the toxin promoted exocytosis of only a small number of SVs in these terminals.

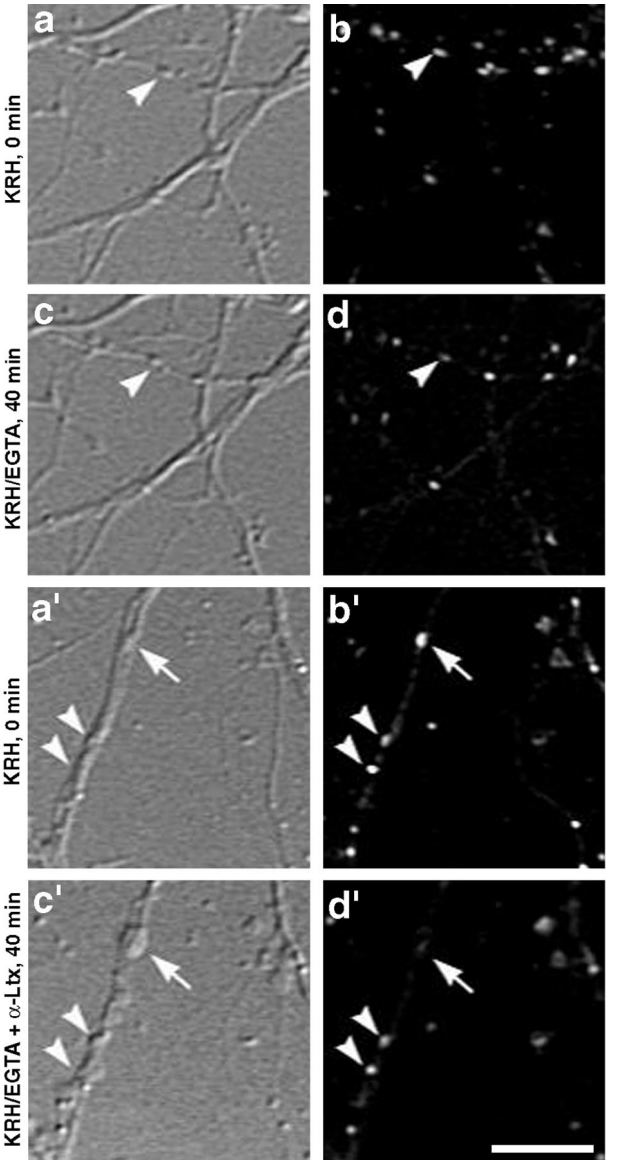

Figure 4. Size of synaptic boutons reflects the extent of α-Ltx–induced exocytosis. Hippocampal neurons (16 DIV) were loaded with FM1-43 during a 90-s incubation in depolarizing solution. DIC (a, c, a′, and c′) and FM1-43 (b, d, b′, and d′) images were recorded at time 0 and after a 40-min incubation in KRH/EGTA in either the absence or presence of 0.1 nM α-Ltx. After toxin treatment, swollen synaptic boutons (arrows in a′ and c′) had released virtually all the dye (compare arrows in b′ and d′), whereas the dye remained in the small synaptic boutons (compare arrowheads in b′ and d′), which were similar in size and brightness to those of the untreated sample (compare arrowheads in b and d). Bar, 10 μm.

When anti-SypI antibodies were applied to α-Ltx–treated neurons before fixation and permeabilization with detergent, bright selective staining of swollen boutons was observed. In contrast, no immunostaining was observed after application of antibodies to synapsin I under the same conditions (Figure 5). The presence of staining for SypI on the

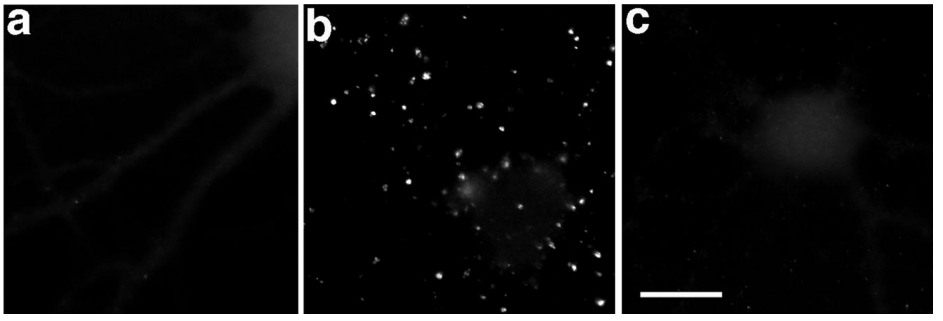

Figure 5. α-Ltx induces SV exocytosis without affecting cell integrity. Hippocampal neurons (15 DIV) were incubated for 5 min in KRH/EGTA in the absence (a) or presence (b and c) of 1 nM α-Ltx. After a 1-h incubation at 37°C with anti-SypI (a and b) or anti-synapsin I (c) antibodies, the cells were fixed and processed for indirect immunofluorescence. Note the bright staining for SypI in the α-Ltx–treated terminals (b), consistent with the notion that some epitopes of the protein become exposed to the extracellular space upon SV fusion (Valtorta *et al*., 1988). The absence of staining for synapsin I (c), a protein associated with the cytosolic side of the SV membrane, indicates that α-Ltx does not lead to damage and permeabilization of the plasma membrane. Bar, 10 μm.

surface of swollen boutons reflects the incorporation of SVs into the plasma membrane as a result of exocytosis, whereas the absence of staining for the cytosolic, SV-associated protein synapsin I indicates that α-Ltx treatment does not lead to cell damage and membrane permeabilization.

The differential effect of α-Ltx on small and swollen boutons could not be ascribed to differences in toxin binding, because incubation of neurons in Ca^{2+}-free medium in the presence of the toxin and a Cy3-conjugated anti-α-Ltx antibody produced similar fluorescent signals for both classes of synaptic boutons (Figure 6).

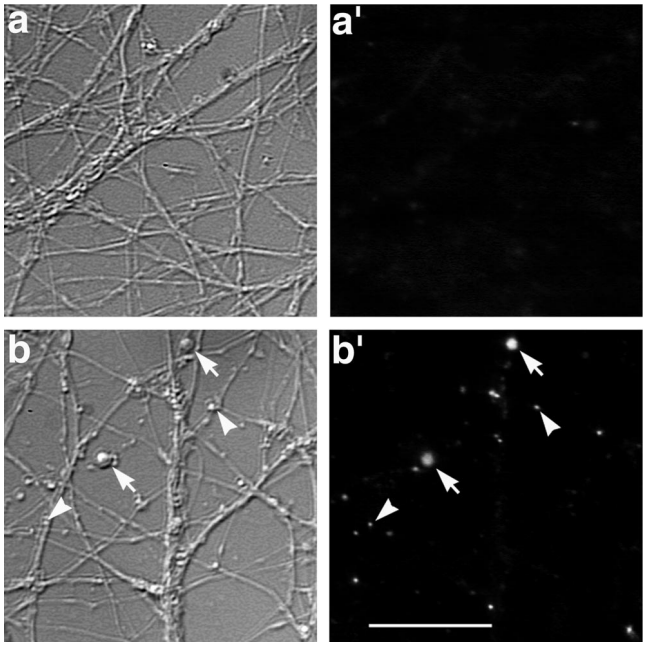

Figure 6. α-Ltx binds to all classes of synaptic boutons. Hippocampal neurons of 16 DIV were incubated for 30 min at 37°C with Cy3-conjugated, anti-α-Ltx antibody in KRH/EGTA in the absence (a and a′) or presence (b and b′) of 0.1 nM α-Ltx. (a and b) differential interference contrast (a′ and b′) fluorescence. Arrows and arrowheads indicate swollen or normally sized synaptic boutons, respectively.

Oligomerization State of Synaptophysin I during Exocytosis

The in vivo study of the molecular interactions between the SV proteins SypI and VAMP2 was carried out by measuring FRET in transfected neurons. Neurons (3 DIV) were cotransfected with fluorescent fusion proteins containing the donor ECFP and the acceptor EYFP, fluorophores, and FRET was measured at 15–18 DIV as donor photobleaching by using time-lapse, video-digital imaging.

To study SypI homo-oligomerization, neurons were cotransfected with the vectors encoding SypI-ECFP and SypI-EYFP. Under resting conditions (KRH/EGTA) FRET efficiency was 24.8 ± 6.4% (mean ± SEM) (Figure 7), indicating that SypI forms homo-oligomers in vivo on the SV membrane. A similar efficiency was measured in the presence of external Ca^{2+} (our unpublished data). To determine whether the oligomerization state of SypI changes during exocytosis, neurons were treated with α-Ltx in the absence of extracellular Ca^{2+}. FRET efficiency within small synaptic boutons remained high (19.4 ± 2.3%), whereas in swollen synaptic boutons FRET efficiency decreased 10-fold to 2.5 ± 0.4%, indicating that the oligomers disassembled upon fusion of SVs with the axolemma. To discriminate FRET on a synapse-by-synapse basis, the average time constants of donor photobleaching were visualized using a pseudocolor scale. Under resting conditions, these time constants were quite heterogeneous, ranging from 10 to 45 s even within single synaptic boutons. After exposure to α-Ltx, the time constants in small synaptic boutons remained heterogeneous and largely similar to those measured under resting conditions. In contrast, in swollen synaptic boutons the time constants dropped below 18 s and were quite homogeneous. Average values ranged from 1 to 9 s among the majority of swollen boutons and among single pixel values within most boutons; only small areas of a minority of boutons had time constants in the range 10–18 s (Figure 8).

The possible role of the COOH-terminal tail of SypI in the assembly of the oligomer was assessed by measuring FRET in neurons expressing SypI fluorescent chimeras lacking the last 73 amino acids. Colocalization of SypIΔC-ECFP with SypI-EYFP and endogenous SV2 confirmed that the deletion mutant was correctly delivered to SVs (our unpublished data). Under resting conditions, FRET efficiency between SypIΔC-ECFP and SypIΔC-EYFP was 19.2 ± 1.6% (n = 3), a value not significantly different from that obtained with the

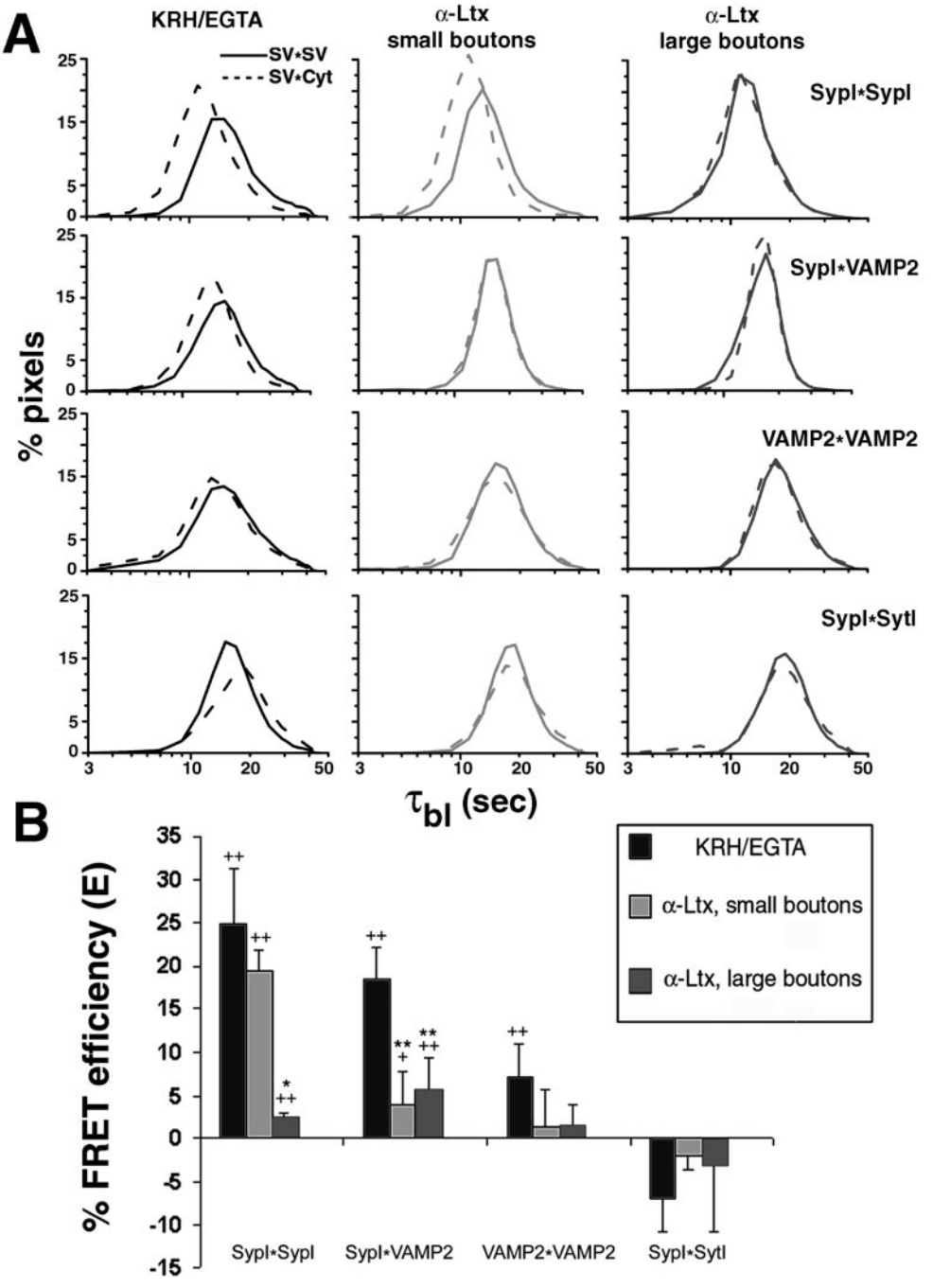

Figure 7. SypI oligomerization and SypI-VAMP2 interaction during exocytosis. FRET measurements were carried out on hippocampal neurons (15–18 DIV) cotransfected with the expression vectors encoding either SypI-ECFP/SypI-EYFP (SypI*SypI), ECFP-VAMP2/SypI-EYFP (SypI*-VAMP2), ECFP-VAMP2/EYFP-VAMP2 (VAMP2*VAMP2), or SypI-ECFP/SytI-EYFP (SypI*SytI). FRET was measured after a 30-min incubation in Ca^{2+}-free medium (KRH/EGTA) in the absence or presence of 0.1 nM α-Ltx. In the toxin-treated samples, normally sized and swollen synaptic boutons were separated for analysis. (A) Distribution of the time constants of donor photobleaching. The results of a typical experiment are shown. SV*SV: samples expressing two fluorescent synaptic vesicle fusion proteins; SV*cyt: control samples expressing one fluorescent synaptic vesicle fusion protein and cytosolic EYFP. For each sample an average of 35,000 pixels was analyzed. (B) FRET efficiencies. SypI*SypI: The changes in FRET efficiencies indicate that SypI is present as a homo-oligomer on the SV membrane and dissociation of the oligomer occurs in α-Ltx–stimulated swollen synaptic boutons, i.e., when the SV completely fuses with the plasma membrane. SypI*VAMP2: The changes in FRET efficiencies indicate that VAMP2 binds to SypI on the SV membrane, and dissociation of VAMP2 from SypI occurs in both α-Ltx–stimulated small and swollen boutons, i.e., before fusion of the SV with the presynaptic membrane. VAMP2*-VAMP2: The changes in FRET efficiencies indicate that VAMP2 molecules interact in vivo to a limited extent, and dissociate in both α-Ltx-stimulated small and swollen boutons, i.e., before fusion. SypI*SytI: The absence of significant FRET indicates that SypI and SytI molecules do not significantly interact in vivo. The negative values of SypI*SytI FRET efficiency under all conditions indicate a slightly higher probability of FRET between SypI-ECFP and cytosolic EYFP than between SypI-ECFP and SytI-EYFP. E values represent means ± SEM from three to five experiments. In each experiment, measurements were carried out on 300-1800 boutons of each class. $^{**}p < 0.01$, $^{*}p < 0.02$, Student's *t* test vs. resting boutons. $++p < 0.01$, $+p < 0.05$, probability that the mean value equals 0 (see MATERIALS AND METHODS).

untruncated protein. This suggests that the COOH-terminal domain is not essential for oligomerization.

When FRET was measured in hippocampal neurons cotransfected with expression vectors encoding ECFP-VAMP2 and EYFP-VAMP2, under resting conditions the FRET efficiency was 7 ± 4%. In toxin-treated neurons, FRET decreased to 1.3 ± 4.5 and 1.5 ± 2.4% in small and swollen synaptic boutons, respectively (Figure 7). Thus, VAMP2 forms few oligomers that dissociate before fusion of SVs.

The specificity of the observed interactions was verified by measuring FRET between SypI and SytI fluorescent pro-

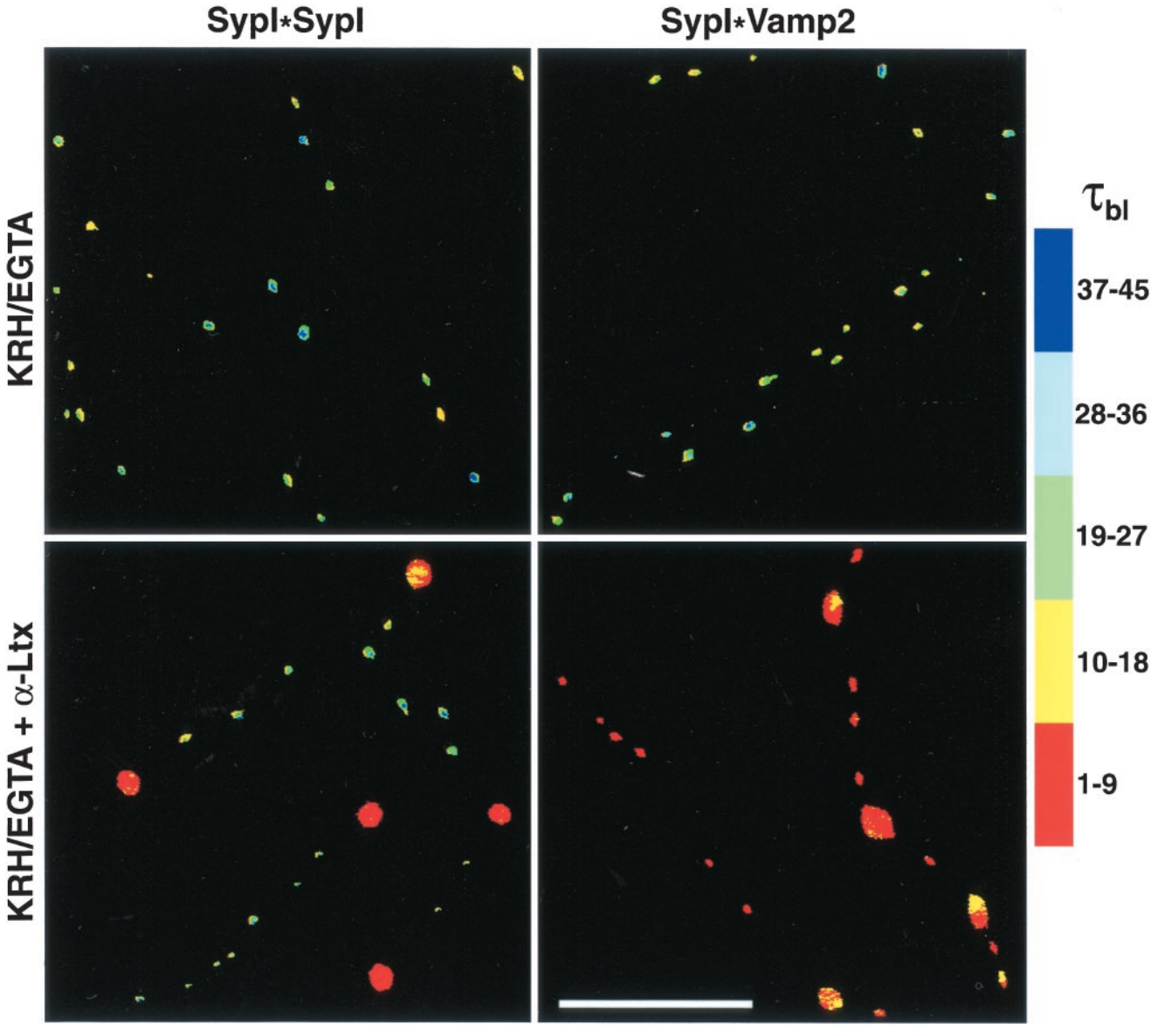

Figure 8. Pseudocolor map of the distribution of the time constants of donor photobleaching. The time constants of donor photobleaching (τ_{bl}) can be depicted in a pseudocolor image (see MATERIALS AND METHODS), allowing a relative evaluation of the spatial and temporal dynamics of protein–protein interactions in living cells. SypI*SypI: Neurons cotransfected with the expression vectors encoding SypI-ECFP and SypI-EYFP. Note the heterogeneity, under resting conditions, of the τ_{bl} values that ranged from 10 to 45 s. Heterogeneity existed not only among synapses, but also within single boutons. After α-Ltx treatment, τ_{bl} values in the class of normally sized synaptic boutons were similar to those of the untreated specimen, whereas in the class of swollen synaptic boutons they were closely grouped in the range of 1–9 s. SypI*VAMP2: Neurons cotransfected with the expression vectors encoding ECFP-VAMP2 and SypI-EYFP. Under resting conditions, the τ_{bl} values ranged from 10 to 45 s, whereas in the α-Ltx–treated sample they decreased to a uniform level in both normally sized and swollen synaptic boutons. Bar, 10 μm.

teins. For this purpose, neurons were cotransfected with SypI-ECFP and SytI-EYFP chimeras. Under resting conditions as well as after α-Ltx treatment, the FRET efficiency was negligible, indicating that no detectable interactions between the two SV proteins occurred either before or after exocytosis (Figure 7).

SypI/VAMP2 Interaction during Exocytosis

The occurrence in vivo of VAMP2 and SypI interaction was evaluated in hippocampal neurons cotransfected with the expression vectors encoding ECFP-VAMP2 and SypI-EYFP. Under resting conditions, the FRET efficiency between SypI and VAMP2 was

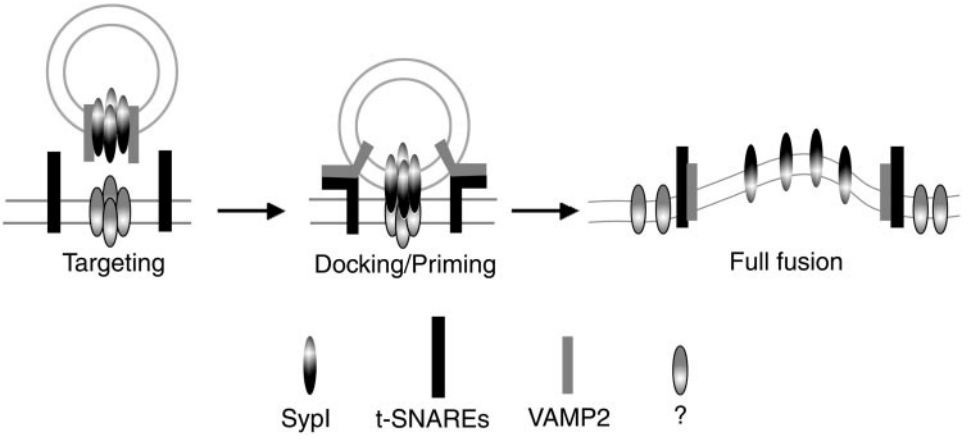

Figure 9. Schematic representation of the changes in SypI-SypI and SypI-VAMP2 interactions occurring during SV exocytosis. Before SV priming, SypI is present as oligomers in the SV membrane and interacts with VAMP2, thus reducing its availability for the formation of the SNARE complexes with the t-SNAREs syntaxin and soluble *N*-ethylmaleimide-sensitive factor attachment protein-25. On priming, but before fusion, VAMP2 is released from SypI oligomers, which may contact a putative presynaptic membrane partner to initiate a fusion pore. The SypI oligomers dissociate only after complete fusion of the SVs with the plasma membrane, after which the monomers function to gather SV components in preparation for endocytotic retrieval.

18.5 ± 3.6% (Figure 7), indicating that in living neurons the two proteins were part of the same complex on the SV membrane. After treatment with α-Ltx, FRET efficiency dropped to 3.9 ± 3.8% in small synaptic boutons and 5.8 ± 3.5% in swollen boutons. The large decrease in FRET efficiency in both swollen and small boutons most simply implies that VAMP2 dissociates from SypI before vesicle fusion.

Pseudocolor images showed that, at rest, the photobleaching time constants were heterogeneous and similar to those observed when FRET was measured between SypI molecules, whereas in α-Ltx–treated samples most time constants in both small and large boutons were in the 1–9-s range, with no time constants >18 s (Figure 8).

The decrease in FRET efficiency observed in the class of swollen synaptic boutons with the tested pairs of fluorescent molecules was not merely the consequence of the dilution of the fluorophores in the axolemma of swollen nerve terminals. In fact, in the interaction between VAMP2 and SypI molecules, FRET occurred to a similar extent in small as well as in swollen boutons. Indeed, in the two classes of boutons, FRET efficiencies were not statistically different from each other ($p > 0.2$), although in both classes they were different from zero ($p < 0.05$).

DISCUSSION

In vivo studies of protein–protein interactions on SVs are hampered by poor accessibility to the small presynaptic compartment. However, by transfecting hippocampal neurons in culture with SV proteins fused to fluorescent proteins and using digital imaging to measure FRET in living neurons, we have, for the first time, directly detected molecular interactions between SV proteins in single synaptic boutons during exocytosis.

To compare protein–protein interactions before and after exocytosis, irreversible fusion of SVs was stimulated by α-Ltx in the absence of external Ca^{2+}, a condition known to cause exocytosis of virtually all SVs present in nerve terminals while blocking their endocytotic retrieval. Under these conditions, collapse of SVs into the plasma membrane results in swelling of nerve terminals (Ceccarelli and Hurlbut, 1980; Valtorta *et al.*, 1988; Torri-Tarelli *et al.*, 1990). However, at the submaximal toxin concentrations used in the present experiments, heterogeneity in the response to the toxin was observed; thus, the areas of many synaptic boutons remained similar to those of control samples, whereas the areas of other swollen boutons increased severalfold.

In cultured hippocampal neurons, the number of SVs per synapse can range from ~20 to >600 (Schikorski and Stevens, 1997). Therefore, α-Ltx–induced swelling may be negligible in boutons containing few SVs. The percentage of synaptic vesicles that had undergone exocytosis in both classes of boutons was established by labeling the recycling SV pool with FM1-43 (Pyle *et al.*, 2000). We found a virtually complete loss of the loaded dye only in synaptic boutons in which α-Ltx had triggered massive exocytosis and an associated swelling. The increase in the size of swollen boutons was consistent with the incorporation of a membrane surface area equivalent to that contributed by 40 to >1000 SVs. In contrast, exocytosis in smaller boutons was limited to a small fraction of SVs, although α-Ltx bound to both classes of boutons.

The high efficiency of FRET between fluorescent SypI molecules in resting terminals as well as in small boutons of α-Ltx–treated terminals indicates that before exocytosis SypI forms homo-oligomers on the SV membrane. These measurements in live neurons extend previous observations that demonstrated that purified SypI is able to form oligomers in vitro (Rehm *et al.*, 1986; Thomas *et al.*, 1988; Johnston and Südhof, 1990). We have also shown that the cytosolic, COOH-terminal domain of the protein is not required for oligomerization. This observation prompts the hypothesis that the process of assembly into a multimeric structure is driven by the highly conserved transmembrane domains, which have been shown to regulate the correct targeting of the protein to small cytoplasmic vesicles in non-neuronal cells (Leube, 1995). A large decrease in FRET efficiency between SypI proteins in α-Ltx–stimulated neurons was observed exclusively in the class of swollen boutons. This provides direct evidence that the oligomerization of SypI is dynamically regulated and that the SypI oligomer disassembles when the SV membrane flattens into the presynaptic membrane.

Similarly, VAMP2 has been reported to form dimers on the SV membrane (Calakos and Scheller, 1994; Washbourne *et al.*, 1995).

We have found VAMP2 proteins interacting on SV membranes in resting nerve terminals, although apparently to a more limited extent than that observed between SypI proteins. Unlike the SypI oligomers, VAMP2 oligomers disassemble before vesicle fusion.

Previously, it has been reported that SypI binds in vitro to VAMP2 and this interaction has been proposed to regulate the availability of VAMP2 for the formation of SNARE complexes (Calakos and Scheller, 1994; Edelmann *et al*., 1995; Washbourne *et al*., 1995). Now, in intact nerve terminals we have observed an interaction between SypI and VAMP2 that is disrupted after α-Ltx treatment. Interestingly, dissociation occurs to similar extents in both swollen and small synaptic boutons, and therefore is not strictly associated with SV exocytosis. Thus, α-Ltx binding seems to alter the molecular arrangement of proteins on the SV membrane before exocytotic fusion.

Similar results were obtained after stimulation of neurotransmitter release with other secretagogues. In particular, taipoxin, a snake toxin that induces massive exocytosis while blocking endocytosis also in the presence of Ca^{2+} (Schiavo *et al*., 2000), gave rise to comparable changes in FRET efficiencies (Rossetto, Pennuto, Valtorta, and Montecucco, unpublished data).

Several hypotheses have been formulated about possible roles played by SypI in neuroexocytosis. Regulation of SNARE complex assembly is based on the sequestration of each component by other factors. Because the SNARE and SypI/VAMP2 complexes seem to be mutually exclusive, SypI might limit VAMP2 availability. Our data are in accordance with the idea that SypI sequesters VAMP2 to prevent SNARE complex assembly in resting terminals (Figure 9). Release of VAMP2 is likely to occur in one of the steps that precede fusion and make SVs competent for exocytosis upon Ca^{2+} influx. We have found that, after α-Ltx treatment, the SypI/VAMP2 complex dissociates in both swollen and small synaptic boutons, consistent with the observation that stable SNARE complexes form during docking and priming (Xia *et al*., 2001). The finding that VAMP2 molecules also interact with each other under resting conditions and dissociate before fusion is consistent with the idea that VAMP2 molecules are monomeric within SNARE complexes (Sutton *et al*., 1998), and raises the possibility that VAMP2 oligomerization represents an additional mechanism for regulating SNARE complex assembly.

Based on the propensity of SypI particles reconstituted into lipid bilayers to form voltage-dependent channels, it has been proposed that SypI is involved in the formation of the fusion pore (Thomas *et al*., 1988), the passageway that transiently connects the SV and the plasma membrane and disassembles after complete fusion has occurred (Monck and Fernandez, 1994). Our finding that SypI oligomers dissociate upon full fusion of SVs is consistent with this hypothesis. However, to form a fusion pore, SypI should presumably bind to a counterpart protein in the plasma membrane, which thus far has not been identified. Because SypI is a major cholesterol-binding protein and oligomerizes, it has been proposed to be responsible for local accumulation of cholesterol, thereby favoring the bending of the planar lipid bilayer necessary for vesicle budding (Thiele *et al*., 2000). This function may be relevant for the generation of precursor vesicles at the level of the *trans*-Golgi network, as well as for the recruitment of lipid and protein components necessary for SV recycling. Indeed, a role for SypI in endocytosis has recently been proposed (Daly *et al*., 2000). The present data support both hypotheses, by showing that SypI is present as an oligomer on the curved SV membrane and dissociates into monomers when the SV membrane collapses into the planar leaflets of the plasmalemma (Figure 9). How the oligomerization process is regulated and at which step of the SV retrieval process SypI reassociates into oligomers remain to be established.

ACKNOWLEDGMENTS

We thank R. Leube (University of Mainz), C. Montecucco (Univesity of Padova), and G.P. Schiavo (Imperial Cancer Research fund, London, Great Britain) for cDNAs; K. Buckley (Harvard University, Cambridge, MA) and R. Jahn (Göttingen, Germany) for the anti-SV2 and anti-SypI monoclonal antibodies, respectively; A. Petrenko (New York University Medical Center) for α-Ltx; R. Fesce for helpful discussions; and J. Meldolesi for critical reading of the manuscript. This work was supported by grants from Telethon (grants 1000 to F.V. and 1131 to F.B.), the Harvard Armenise Foundation and Ministry of Education, Universities and Research (University Excellence Center on Physiopathology of Cell Differentiation to F.V. and PRIN MM05274413 to F.B.).

REFERENCES

Alder, J., Kanki, H., Valtorta, F., Greengard, P., and Poo, M.-M. (1995). Overexpression of synaptophysin enhances neurotransmitter secretion at *Xenopus* neuromuscular synapses. J. Neurosci. *15*, 511–519.

Alder, J., Lu, B., Valtorta, F., Greengard, P., and Poo, M.-M. (1992a). Calcium-dependent transmitter secretion reconstituted in *Xenopus* oocytes. Science *257*, 657–661.

Alder, J., Xie, Z.P., Valtorta, F., Greengard, P., and Poo, M.-M. (1992b). Antibodies to synaptophysin interfere with transmitter secretion at neuromuscular synapses. Neuron *9*, 759–768.

Banker, G., and Cowan, W. (1977). Rat hippocampal neurons in dispersed cell culture. Brain Res. *13*, 397–342.

Bajjalieh, S.M., Frantz, G.D., Weimann, J.M., McConnel, S.K., and Scheller, R.H. (1994). Differential expression of synaptic vesicle protein 2 (SV2) isoforms. J. Neurosci. *14*, 5223–5235.

Baumert, M., Maycox, P.R., Navone, F., De Camilli, P., and Jahn, R. (1989). Synaptobrevin: an integral membrane protein of 18,000 daltons present in small synaptic vesicles of rat brain. EMBO J. *8*, 379–384.

Baumert, M., Takei, K., Hartinger, J., Burger, P.M., Fischer von Mollard, G., Maycox, P.R., De Camilli, P., and Jahn, R. (1990). P29: a novel tyrosine-phosphorylated membrane protein present in small clear vesicles of neurons and endocrine cells. J. Cell Biol. *110*, 1285–1294.

Benfenati, F., Onofri, F., and Giovedì, S. (1999). Protein-protein interactions and protein modules in the control of neurotransmitter release. Phil. Trans. R. Soc. Lond. B *354*, 243–257.

Betz, W.J., Mao, F., and Smith, C.B. (1996). Imaging exocytosis and endocytosis. Curr. Opin. Neurobiol. *6*, 365–371.

Buckley, K.M., Floor, E., and Kelly, R. (1987). Cloning and sequence analysis of cDNA encoding p38, a major synaptic vesicle protein. J. Cell Biol. *105*, 2447–2456.

Calakos, N., and Scheller, R.,. (1994). Vesicle-associated membrane protein and synaptophysin are associated on the synaptic vesicle. J. Biol. Chem. *269*, 24534–24537.

Ceccarelli, B., and Hurlbut, W.P. (1980). Ca^{2+}-dependent recycling of synaptic vesicles at the frog neuromuscular junction. J. Cell Biol. *87*, 297–303.

Daly, C., Sugimori, M., Moreira, J.E., Ziff, E.B., and Llinás, R. (2000). Synaptophysin regulates clathrin-independent endocytosis of synaptic vesicles. Proc. Natl. Acad. Sci. USA *97*, 6120–6125.

Edelmann, L., Hanson, P.I., Chapman, E.R., and Jahn, R. (1995). Synaptobrevin binding to synaptophysin: a potential mechanism for controlling the exocytotic fusion machine. EMBO J. *14*, 224–231.

Elferink, L.A., Trimble, W.S., and Scheller, R.H. (1989). Two vesicle-associated membrane protein genes are differentially expressed in rat central nervous system. J. Biol. Chem. *264*, 11061–11064.

Eshkind, L.G., and Leube, R.E. (1995). Mice lacking synaptophysin reproduce and form typical synaptic vesicles. Cell Tissue Res. *282*, 423–433.

Jahn, R., Scheibler, W., Ouimet, C., and Greengard, P. (1985). A 38,000 dalton membrane protein (p38) present in synaptic vesicles. Proc. Natl. Acad. Sci. USA *82*, 4137–4141.

Janz, R., and Südhof, T. (1998). Cellugyrin, a novel ubiquitous form of synaptogyrin that is phosphorylated by pp60c-src. J. Biol. Chem. *273*, 2851–2857.

Janz, R., Südhof, T.C., Hammer, R.E., Unni, V., Siegelbaum, S.A., and Bolshakov, V.Y. (1999). Essential roles in synaptic plasticity for synaptogyrin I and synaptophysin I. Neuron *24*, 687–700.

Johnston, P.A., and Südhof, T.C. (1990). The multisubunit structure of synaptophysin. J. Biol. Chem. *265*, 8869–8873.

Jovin, T.M., and Arndt-Jovin, D. (1989). FRET microscopy: digital imaging of fluorescence resonance energy transfer. In: Application in Cell Biology. Cell Structure and Function by Microspectrofluorimetry, ed. E. Kohen and J.G. Hirschberg), San Diego: Academic Press, 99–117.

Kingston, R.E. (1997). Current Protocols in Molecular Biology, New York: John Wiley & Sons, 9.0.1–9.0.5.

Knaus, P., Marquèze-Pouey, B., Scherer, H., and Betz, H. (1990). Synaptoporin, a novel putative channel protein of synaptic vesicles. Neuron *5*, 453–462.

Kosik, K.S., and Finch, E.A. (1987). MAP2 and tau segregate into dendritic and axonal domains after the elaboration of morphologically distinct neurites: an immunocytochemical study of cultured rat cerebrum. J. Neurosci. *7*, 3142–3153.

Leube, R.E. (1994). Expression of the synaptophysin gene family is not restricted to neuronal and neuroendocrine differentiation in rat and human. Differentiation *56*, 163–171.

Leube, R.E. (1995). The topogenic fate of the polytopic transmembrane proteins, synaptophysin and connexin, is determined by their membrane-spanning domains. J. Cell Sci. *108*, 883–894.

Leube, R.E., *et al*. (1987). Synaptophysin: molecular organization and mRNA expression as determined from cloned cDNA. EMBO J. *6*, 3261–3268.

McMahon, H.T., Bolshakov, V.Y., Janz, R., Hammer, R.E., Siegelbaum, S.A., and Südhof, T.C. (1996). Synaptophysin, a major synaptic vesicle protein, is not essential for neurotransmitter release. Proc. Natl. Acad. Sci. USA *93*, 4760–4764.

Menegon, A., Dunlap, D.D., Castano, F., Benfenati, F., Czernik, A.J., Greengard, P., and Valtorta, F. (2000). Use of phosphosynapsin I-specific antibodies for image analysis of signal transduction in single nerve terminals. J. Cell Sci. *113*, 3573–3582.

Monck, J.R., and Fernandez, J.M. (1994). The exocytotic fusion pore and neurotransmitter release. Neuron *12*, 707–716.

Nakata, T., Terada, S., and Hirokawa, N. (1998). Visualization of the dynamics of synaptic vesicle and plasma membrane proteins in living axons. J. Cell Biol. *140*, 659–674.

Pelham, H.R.B. (2001). SNAREs and the specificity of membrane fusion. Trends Cell Biol. *11*, 99–101.

Pyle, J.L., Kavalali, E.T., Piedras-Renteria, E.S., and Tsien, R. (2000). Rapid reuse of readily releasable pool vesicles at hippocampal synapses. Neuron *28*, 221–231.

Rehm, H., Wiedenmann, B., and Betz, H. (1986). Molecular characterization of synaptophysin, a major calcium-binding protein of the synaptic vesicle membrane. EMBO J. *5*, 535–541.

Schiavo, G., Matteoli, M., and Montecucco, C. (2000). Neurotoxins affecting neuroexocytosis. Physiol. Rev. *80*, 717–766.

Schikorski, T., and Stevens, C.F. (1997). Quantitative ultrastructural analysis of hippocampal excitatory synapses. J. Neurosci. *17*, 5858–5867.

Shibaguchi, H., Takemura, K., Kan, S., Kataoka, Y., Kaibara, M., Saito, N., and Taniyama, K. (2000). Role of synaptophysin in exocytotic release of dopamine from *Xenopus* oocytes injected with rat brain mRNA. Cell Mol. Neurobiol. *20*, 401–408.

Söllner, T., Bennett, M.K., Whiteheart, S.W., Scheller, R.H., and Rothman, J.E. (1993). A protein assembly-disassembly pathway in vitro that may correspond to sequential steps of synaptic vesicle docking, activation, and fusion. Cell *75*, 409–418.

Südhof, T.C. (1995). The synaptic vesicle cycle: a cascade of protein-protein interaction. Nature *375*, 488–493.

Südhof, T.C., Lottspeich, F., Greengard, P., Mehl, E., and Jahn, R. (1987). A synaptic vesicle protein with a novel cytoplasmic domain and four transmembrane regions. Science *238*, 1142–1144.

Sugita, S., Janz, R., and Südhof, T.C. (1999). Synaptogyrins regulate Ca^{2+}-dependent exocytosis in PC12 cells. J. Biol. Chem. *274*, 18893–18901.

Sutton, R.B., Fasshauer, D., Jahn, R., and Brunger, A. (1998). Crystal structure of a SNARE complex involved in synaptic exocytosis at 2.4 Å resolution. Nature *395*, 347–353.

Thiele, C., Hannah, M.J., Fahrenholz, F., and Huttner, W.B. (2000). Cholesterol binds to synaptophysin and is required for biogenesis of synaptic vesicles. Nat. Cell Biol. *2*, 42–49.

Thomas, L., Hartung, K., Langosch, D., Rehm, H., Bamberg, E., Franke, W.W., and Betz, H. (1988). Identification of synaptophysin as a hexameric channel protein of the synaptic vesicle membrane. Science *242*, 1050–1053.

Torri-Tarelli, F., Villa, A., Valtorta, F., De Camilli, P., Greengard, P., and Ceccarelli, B. (1990). Redistribution of synaptophysin and synapsin I during α-latrotoxin-induced release of neurotransmitter at the neuromuscular junction. J. Cell Biol. *110*, 449–459.

Tsien, R.Y. (1998). The green fluorescent protein. Annu. Rev. Biochem. *67*, 509–544.

Valtorta, F., and Benfenati, F. (1995). Membrane trafficking in nerve terminals. Adv. Pharmacol. *32*, 505–557.

Valtorta, F., Jahn, R., Fesce, R., Greengard, P., and Ceccarelli, B. (1988). Synaptophysin (p38) at the frog neuromuscular junction: its incorporation into the axolemma and recycling after intense quantal secretion. J. Cell Biol. *107*, 2719–2730.

Valtorta, F., and Leoni, C. (1999). Molecular mechanisms of neurite extension. Phil. Trans. R. Soc. Lond. B. *354*, 387–394.

Valtorta, F., Meldolesi, J., and Fesce, R. (2001). Synaptic vesicles: is kissing a matter of competence? Trends Cell Biol. *11*, 323–327.

Washbourne, P., Schiavo, G., and Montecucco, C. (1995). Vesicle-associated membrane protein-2 (synaptobrevin-2) forms a complex with synaptophysin. Biochem. J. *305*, 721–724.

Wiedenmann, B., and Franke, W.W. (1985). Identification and localization of synaptophysin, an integral membrane glycoprotein of M_r 38,000 characteristic of presynaptic vesicles. Cell *41*, 1017–1028.

Xia, Z., Zhou, Q., Lin, J., and Liu, Y. (2001). Stable SNARE complex prior to evoked synaptic vesicle fusion revealed by fluorescence resonance energy transfer. J. Biol. Chem. *276*, 1766–1771.